Plant Molecular Biology (2022) 108:93–103
https://doi.org/10.1007/s11103-021-01227-8

Potent inhibition of TCP transcription factors by miR319 ensures proper root growth in Arabidopsis

Julia L. Baulies[1] · Edgardo G. Bresso[1] · Camila Goldy[1] · Javier F. Palatnik[1,2] · Carla Schommer[1,2]

Received: 10 June 2021 / Accepted: 22 November 2021 / Published online: 4 January 2022

Abstract

Key message **Proper root growth depends on the clearance of TCP transcripts from the root apical meristem by microRNA miR319.**

Abstract The evolutionarily conserved microRNA miR319 regulates genes encoding TCP transcription factors in angiosperms. The miR319-TCP module controls cell proliferation and differentiation in leaves and other aerial organs. The current model sustains that miR319 quantitatively tunes TCP activity during leaf growth and development, ultimately affecting its size. In this work we studied how this module participates in Arabidopsis root development. We found that misregulation of TCP activity through impairment of miR319 binding decreased root meristem size and root length. Cellular and molecular analyses revealed that high TCP activity affects cell number and cyclin expression but not mature cell length, indicating that, in roots, unchecking the expression of miR319-regulated TCPs significantly affects cell proliferation. Conversely, *tcp* multiple mutants showed no obvious effect on root growth, but strong defects in leaf morphogenesis. Therefore, in contrast to the quantitative regulation of the TCPs by miR319 in leaves, our data suggest that miR319 clears TCP transcripts from root cells. Hence, we provide new insights into the functions of the miR319-TCP regulatory system in Arabidopsis development, highlighting a different *modus operandi* for its action mechanism in roots and shoots.

Keywords microRNA miR319 · TCP transcription factors · Root apical meristem · Quiescent center · *Arabidopsis thaliana*

Introduction

The TCPs are a plant-specific transcription factor family characterized by a motif, the TCP domain, which is predicted to fold into a basic helix-loop-helix structure known from DNA-binding domains of both plant and animal transcription factors (Cubas et al. 1999). The family is named after the first identified members: TEOSINTE BRANCHED1 from maize, CYCLOIDEA from snapdragon, and the two PCNA promoter binding factors PCF1 and PCF2 from rice [reviewed in (Cubas et al. 1999; Martin-Trillo and Cubas 2010)]. Arabidopsis has 24 TCPs, classified in two main branches (classes I and II) according to the sequence of their TCP domain, which fulfill various important roles in plant development [reviewed in (Martin-Trillo and Cubas 2010; Danisman et al. 2013; Li 2015)].

In Arabidopsis, five closely related class II *TCPs*, namely *TCP2*, *TCP3*, *TCP4*, *TCP10* and *TCP24*, contain a target site for microRNA miR319 (Palatnik et al. 2003) located outside the TCP domain, closer to the 3' part of the coding region. Within these, two subgroups can be identified

Julia L. Baulies and Edgardo G. Bresso have contributed equally to this work and share first authorship.

✉ Carla Schommer
schommer@ibr-conicet.gov.ar

Julia L. Baulies
baulies@ibr-conicet.gov.ar

Edgardo G. Bresso
egbresso@gmail.com

Camila Goldy
goldy@ibr-conicet.gov.ar

Javier F. Palatnik
palatnik@ibr-conicet.gov.ar

[1] Instituto de Biología Molecular y Celular de Rosario, Ocampo y Esmeralda s/n, 2000 Rosario, Argentina

[2] Centro de Estudios Interdisciplinarios (CEI), Universidad Nacional de Rosario, Maipú 1065, 2000 Rosario, Argentina

according to sequence similarity, one comprised by *TCP3*, *TCP4* and *TCP10*, the other by *TCP2* and *TCP24* (Citerne et al. 2003; Li 2015). Plants with reduced activity of these genes, such as loss-of-function mutants and the miR319-overexpressing *jaw*-D mutant have larger leaves (Palatnik et al. 2003; Efroni et al. 2008; Schommer et al. 2008; Koyama et al. 2010; Bresso et al. 2018). On the contrary, those with increased class II TCP activity have smaller leaves (Palatnik et al. 2003; Koyama et al. 2010; Schommer et al. 2014). Such is the case of the *suppressor of jaw-D 8* (*soj8*) mutant which was isolated from an ethyl methanesulfonate mutagenesis screen (Palatnik et al. 2007) and harbors a point mutation in the miR319 target site, acquiring partial resistance to microRNA regulation. Analyses of these mutants with altered TCP activity, as well as transgenic lines carrying artificial microRNAs, suggest that class II TCPs are key factors that connect the developmental program with basic mechanisms of the cell cycle, and ultimately show that the miR319-TCP regulatory node participates in different aspects throughout leaf development, from cell proliferation at early stages, through cell differentiation, to senescence at the end of its life. However, although there is considerable knowledge on the nature of this regulation in the shoot, little is known about the role of miR319-regulated TCPs in root development.

The root apical meristem (RAM) contains the quiescent center (QC), a group of cells that seldom divide and contribute to maintain a group of surrounding stem cells. These originate the cell types that constitute the different root cell layers, i.e., stele, pericycle, endodermis, cortex, epidermis, lateral root cap cells and columella. Initially, each cell type amplifies in number by mitosis and eventually starts elongation and differentiation in the transition zone, which is located at the proximal end of the RAM. [reviewed in (Petricka et al. 2012)].

RAM architecture and function rely on plant hormones. For example, the antagonistic interplay between auxin and cytokinin establishes RAM size, and upon its wounding, local jasmonic acid (JA) accumulation leads to the activation of CYCD6;1, stimulating divisions of QC cells and promoting regeneration (Zhou et al. 2019b). Also, exogenously applied JA inhibits primary root growth, reducing cell proliferation and elongation, and altering RAM morphology (Chen et al. 2011). Most conspicuously, some of the validated target genes of the miR319-regulated TCPs are involved in either hormone biogenesis or signaling. For instance, they directly activate the promoters of genes involved in auxin-cytokinin interaction, like *SMALL AUXIN UP REGULATED 65* and *INDOLE-3-ACETIC ACID INDUCIBLE/SHORT HYPOCOTYL 2* (*IAA3/SHY2*) (Koyama et al. 2010). Gain-of-function *shy2-2* mutants have larger cotyledons and altered auxin-dependent root development, resulting in shorter roots (Tian et al. 2002). More specifically, *SHY2* contributes to maintain the size of the root meristematic zone (Dello Ioio et al. 2008; Weigel and Glazebrook 2009). Additionally, several JA biosynthesis genes have TCP-binding sites in their promoters and respond to altered miR319 or TCP4 levels (Schommer et al. 2008). Among them is *LIPOXYGENASE2* (*LOX2*) which catalyzes the first dedicated step in the biosynthesis of the oxylipin JA, and has at least two validated TCP4-binding sites (Bell et al. 1995; Schommer et al. 2008).

Despite the many advances in understanding gene regulatory networks involving the TCP transcription factors, much of the molecular complexity inherent to them remains to be elucidated. Here, we characterize a so far unknown role of miR319 in the Arabidopsis root. We demonstrate that impairing the miR319-driven control of TCP activity significantly affects root growth and root meristem architecture. Furthermore, we show that miR319 is a potent inhibitor of TCP activity in roots that qualitatively eliminates *TCP* transcripts from the meristematic zone. Our results provide new insights to the importance of this microRNA regulatory node in Arabidopsis development and reveal different functioning modes in roots and leaves.

Materials and methods

Plant material and growth conditions

Arabidopsis thaliana accession Col-0 was used throughout this study. See Supplemental Table S1 for a list and description of the transgenic lines used. Origins of *soj8* and *tcp* mutant lines and the transgenic marker line *promAGL42:GFP* and *DR5:3xVENUS-N7* have been described before (Heisler et al. 2005; Nawy et al. 2005; Palatnik et al. 2007; Schommer et al. 2008; Bresso et al. 2018).

Plants were grown in growth cabinets at 23 °C under long day conditions (16 h light/8 h dark). Regular illumination was 125 µmol m^{-2} s^{-1}. Plants were grown vertically in square plates (125 × 125 × 15 mm) on plant growth medium: 1 × Murashige and Skoog (MS) salt mixture, 1% W/V sucrose, and 2.3 mM 2-(N-morpholino) ethanesulfonic acid (MES), pH 5.8, in 1% W/V plant cell culture tested agar. Kanamycin was added at 50 µg/l for the selection of T1 plants, stable lines were grown without kanamycin.

Root length measurements

Plates were placed vertically in a growth cabinet after two days of stratification at 4 °C. On the first day after germination (DAG) the position of the root tip for each plant in the plate was recorded by marking a dot with a permanent marker at Zeitgeber time 6. On consecutive days a new dot

was recorded at the same time. Plates were photographed with a digital camera. Images were analyzed using open-source Fiji software (Schindelin et al. 2012). Briefly, for each plant, the trail of the root between each of the marked dots was measured and recorded. The mean and standard error for each time point and genotype is shown in the corresponding line plots.

Confocal microscopy and phenotypic analyses

Plant material was visualized under a Zeiss LSM880 confocal scanning microscope, using the 488-nm laser line for excitation, a 515/30-nm band-pass filter for GFP detection, and a 605/75-nm band-pass filter for propidium iodide detection. Images were acquired after staining the roots with 10 µg/ml propidium iodide in water. Determination of the root meristematic zone length was performed by measuring the distance from the base of the QC up to the cell in the cortex file that is twice the length of the immediately preceding cell (Ercoli et al. 2018a). The number of cortex cells between those two points was recorded as the cortex cell number in the meristematic zone. Length of fully elongated (mature) cortex cells was measured in cells located five optical fields shootward from the end of the meristematic zone towards the plant apex. The number of analyzed plants for each genotype is indicated in text.

Confocal images of roots were obtained at five days after germination (DAG).

Fluorescence intensity measurements were performed as described before (Ercoli et al. 2018a).

Sample collection for gene expression analyses

Plants were grown on vertical square plates and their elongation recorded as described in the previous section. On the fifth DAG, the elongated portion of the root tip from the previous 24 h was dissected and collected in a tube in liquid nitrogen, from 50 individuals per replicate (sample "root"). From the same individuals, the apices were dissected by removing the hypocotyl and cotyledons and collected inside a second tube (sample "shoot"). Four biological replicates were collected.

Expression analyses

For real time quantitative polymerase chain reaction (RT-qPCR) assays, RNA was extracted using TRIzol reagent (Invitrogen), and 0.5 µg of total RNA was treated with RQ1 RNase-free DNase (Promega). First-strand cDNA synthesis was carried out using SuperScriptTM III Reverse Transcriptase (Invitrogen) with the appropriate primers. PCR reactions were performed in a Mastercycler ep realplex thermal cycler (Eppendorf) using SYBR-Green I (Roche) to monitor dsDNA synthesis. Relative transcript levels were determined for each sample and normalized to *PROTEIN PHOSPHATASE 2A* levels. Mature miR319 levels were determined by stem-loop RT-qPCR (Chen et al. 2005). Primer sequences are the following: *CYCB1;2*: TCCCTC CATGCTTGCTGCTTC; CCTGCTCTCACCGCATCTC; *LOX2*: AGGACTCATGCCTGTACGGAGCCA; CCATGT TCTGCGGTCTTATCTTCC; miR319: specific RT oligo: GTTGGCTCTGGCAGGTCCGAGGTATCGCCAGAGCCA ACA(G/A)GGAG; GCGGCGGTTGGACTGAAGGGAG; TTGGCTCTGGCAGGTCCGAGGT; *PP2A*: CCTGCGGTA ATAACTGCATCT; CTTCACTTAGCTCCACCAAGCA; *SHY2*: GGTGCACCATACTTGAGGAAA; CAACCCAAG CACAGACAGAGAT *TCP4*: AGCAACCGATACAGGAAA CGGA; TGAGGATCAAACCAAGCACGGA.

To visualize reporter activity, transgenic plants were subjected to GUS staining (n = 25 for each genotype) similar as described by (Donnelly et al. 1999). Briefly, roots were placed in 90% acetone on ice for 15 min, and then incubated for 16 h in X-Gluc buffer solution (750 mg/ml X-Gluc, 100 mM, NaPO4 (pH 7), 3 mM K3F3(CN)6, 10 mM EDTA, 0.1% Tween).

Plasmid construction and generation of transgenic lines

Transgenic constructs were generated by introducing *TCP2* and *TCP4* cDNAs (wild-type and miR319 resistant versions) as *Bam*HI/*Sal*I fragments from previous published vectors (Palatnik et al. 2003) into CHF3 binary vector backbone (Jarvis et al. 1998). *GFP* was introduced to the same vector as *Sal*I/*Pst*I fragment. In the case of the *promTCP4:TCP4:GFP* constructs the *35S* promoter of CHF3 was replaced by 2.3 kb of *TCP4* promoter sequences, introduced as *Mun*I/*Kpn*I fragment. Table S1 visualizes the wild type miR319 target site in *TCP2* and *TCP4*, as well as the silent mutations in the miR319 target site of the microRNA-resistant (r) versions. Binary constructs were introduced into *A. tumefaciens* strain: ASE. Arabidopsis plants, accession Col-0 were transformed by floral dip (Clough and Bent 1998).

Results

miR319-regulation of TCP4 is necessary for proper root growth

In the shoot, high levels of microRNA-regulated TCPs dramatically affect plant morphology (Palatnik et al. 2003; Efroni et al. 2008; Koyama et al. 2010; Schommer et al. 2014; Bresso et al. 2018), but their importance in root growth has not been addressed so far. Here, we set out to

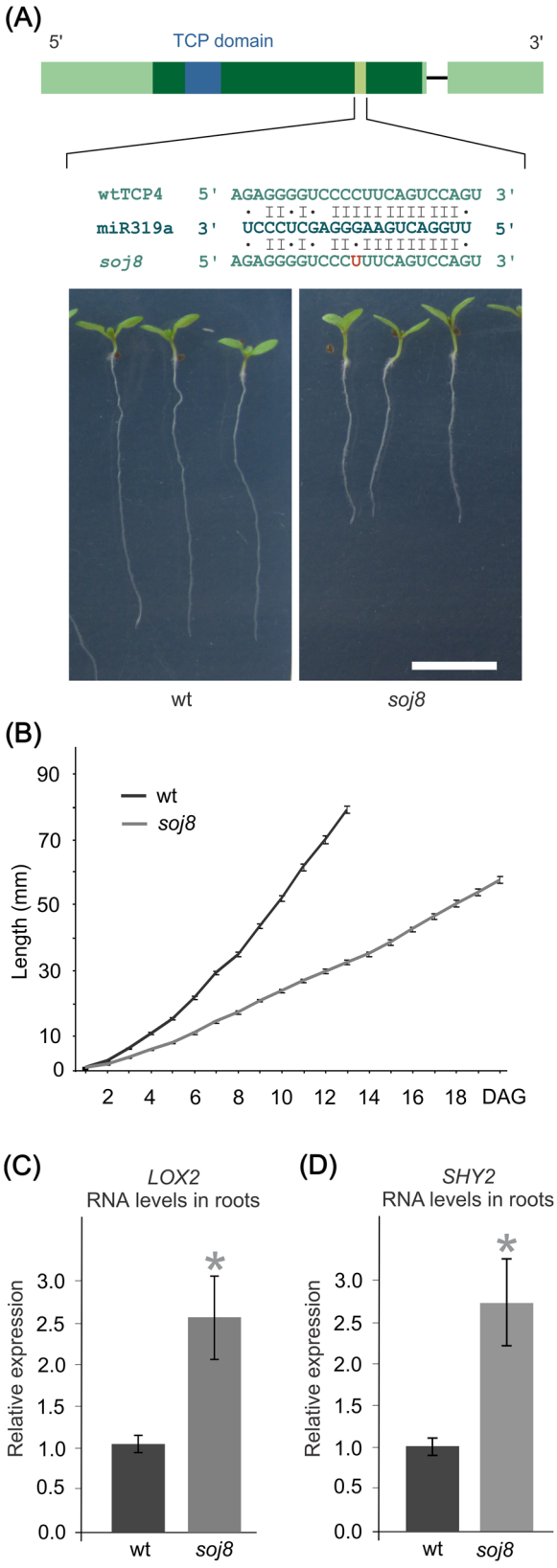

Fig. 1 Unchecking miR319 control from *TCP4* inhibits root growth and increases target gene expression. **a** Schematic representation of *TCP4*. Intron indicated as black line; exons, as boxes; untranslated regions, in light green; the *TCP* domain, in blue; and the miR319 target site, in olive green. Below are the *TCP4* target sequences in wild-type and the *soj8* mutant. The images are from seedlings grown vertically for five days, showing the shorter roots of *soj8* compared to wild type.; scale bar: 1cm. **b** Average root length for wild-type (wt) and *soj8* mutant line (n = 25 each line); x-axis is days after germination (DAG). Error bars depict standard error. **c** Relative *LOX2* RNA levels in wt and *soj8* roots. **d** Relative *SHY2* RNA levels in wt and *soj8* roots. Asterisks in (**c**) and (**d**) indicate significant differences from wild type (Student's t-test, $p < 0.01$)

investigate the importance of miR319 regulation of TCP4 in the Arabidopsis root. The *suppressorofjaw-D 8* (*soj8)* line was identified earlier in an ethyl methanesulfonate-screen and harbors a single-nucleotide mutation in position 11 of the miR319-binding site of *TCP4*, which affects microRNA-guided cleavage of its mRNA and therefore increases its in vivo transcript levels (Fig. 1a) (Palatnik et al. 2007). We observed that *soj8* roots grew slower than wild-type ones in the first days after germination (Fig. 1a, b). In addition, we compared the transcript levels of *LOX2* and *SHY2* as examples of known targets of miR319-regulated TCPs (Schommer et al. 2008; Koyama et al. 2010). In the root of the *soj8* mutant, the transcript levels of both, *LOX2* and *SHY2,* increased more than two-fold compared to wildtype plants (Fig. 1c, d), which is consistent with higher TCP activity. We also analyzed root growth of transgenic plants expressing a microRNA-resistant version of *TCP4* (*rTCP4*) under its endogenous promoter (*promTCP:rTCP4:GFP*). As these generally have severe developmental defects and do not set seeds (Palatnik et al. 2003), we assessed primary transformants. In all but one line root growth was reduced in comparison to an empty vector control (Fig. S1) endorsing the idea that diminishing miR319-driven control of *TCP4* leads to reduced root growth in Arabidopsis.

Unchecking miR319-regulation of TCP4 reduces RAM size

Alterations in root length can be caused by a change in the number of cells, by cell elongation defects, or by a combination of both (Lucas and Shaw 2012; Wen et al. 2013; Bao et al. 2014; Ercoli et al. 2018b). Therefore, to establish the cause of the *soj8* mutant phenotype we analyzed the RAM at the cellular level using laser scanning confocal microscopy (Fig. 2a). Analyzing 20 individuals for each genotype we found that *soj8* mutants presented a shorter meristematic zone (MZ) with fewer cortex cells in comparison to the wild type (Fig. 2a, b). However, we observed no significant difference in the final length of cortex cells between wild-type and mutant lines (Fig. 2b). These results indicated that the short root phenotype of *soj8* plants with its increased levels

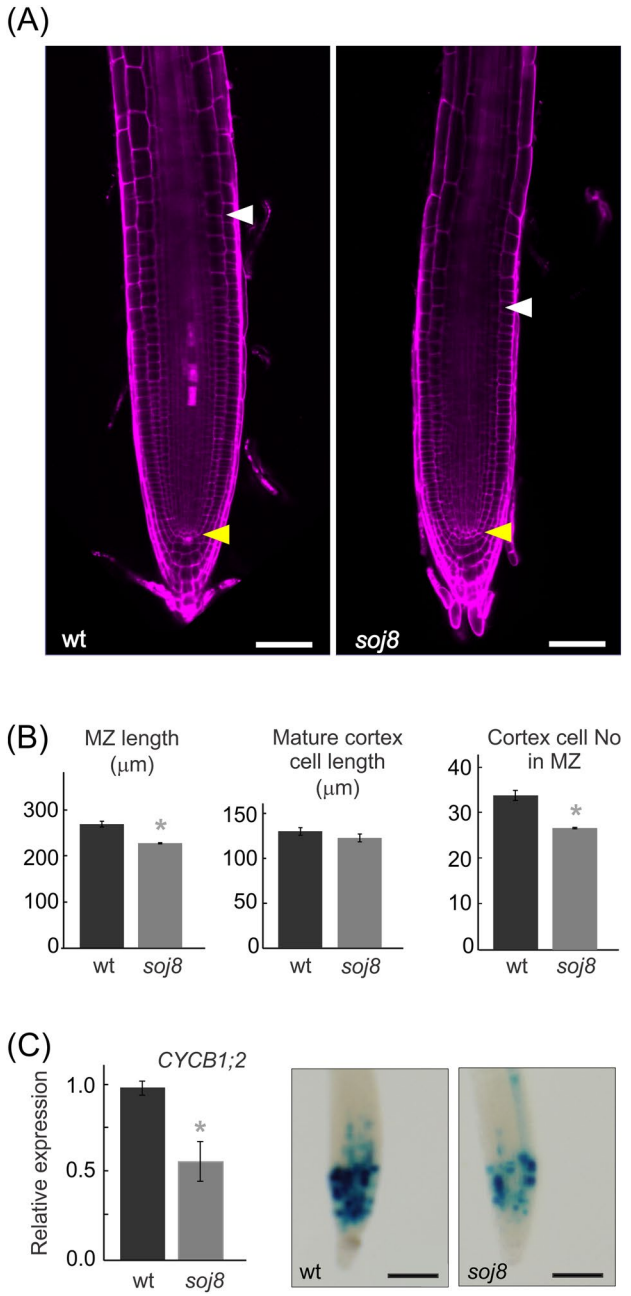

Fig. 2 miR319 controls root apical meristematic size through regulation of *TCP4*. **a** Representative confocal images of propidium iodide-stained (magenta) wt and *soj8* roots (n = 50) five days after germination; white arrowheads indicate the end of the meristematic zone, and yellow ones mark the QC (scale bar: 50µm). **b** Analysis of the meristematic zone (MZ) length (left panel), y-axis in µm; length of mature cortex cells (middle panel), y-axis in µm and number (No) of cortex cells in the meristematic zone (MZ) (right panel). Error bars depict standard error and asterisks indicate significant differences from wt (Student's t-test, $p < 0.01$). **c** Left panel: relative transcript levels of *CYCLINB1; 2* in wt and *soj8* mutant roots, asterisk indicates significant difference from wildtype as determined by Student's t-test ($p < 0.01$); right panel: β-glucoronidase assay in wt and *soj8* roots expressing a CYCLINB1;1-GUS reporter. Images representative of 25 individuals for each line. Scale bar: 0.1 mm

of *TCP4* is due to a defect in cell proliferation rather than cell elongation.

Next, we crossed *soj8* plants with a CYCB1;1-GUS reporter line to assess the proliferative capacity of the RAM. CYCB1;1 participates in the control of the G2/M transition of the cell cycle and marks actively dividing cells in the meristem (Colon-Carmona et al. 1999). Histological GUS staining showed a slight decrease in CYCB1;1 activity (Fig. 2c) and, in addition, RT-qPCR of RNA extracted from root tips (encompassing the whole MZ) revealed significantly lower *CYCB1;2* transcript levels in the mutant background compared with the wild-type plants (Fig. 2c).Taken together, these results not only correlate with the phenotypes observed at the whole organ level, but also allow us to conclude that the short length of the *soj8* mutant root is due to a reduction in the number of cells, reflecting a lower proliferative activity of the RAM.

miR319 activity guarantees proper RAM organization

A closer inspection of the median longitudinal optical sections of *soj8* roots revealed that a high proportion of individuals had an abnormal RAM (Figs. 3a, b, S2), with alterations in cell morphology and arrangement, the QC being the most affected (43 of 61 analyzed individuals). In contrast, almost all wild-type QCs were normal (23 of 25 analyzed individuals). We crossed the *soj8* mutant to an AGL42 reporter (*promAGL42:GFP*) which is expressed in the QC and the surrounding stele and ground tissue (Nawy et al. 2005). Consistent with a morphologically altered stem cell niche, we found a lower and irregular GFP signal in *soj8* background, without the hallmark strong fluorescent expression that is seen for the QC central cells in wild type (Figs. 3c, d; S3). We also crossed the *soj8* mutant to the auxin reporter line *DR5:3xVENUS-N7* (Heisler et al. 2005), and observed that the fluorescent signal was reduced in the mutant background (Figs. 3e, f; S4), indicating a possible disturbance of the auxin homeostasis in the mutant root.

Next, we set out to analyze the expression pattern of TCP4 in the root. We analyzed T1 individuals of two reporter constructs in which a wild-type and a microRNA-resistant version of this transcription factor were fused to GFP under control of the endogenous TCP4 promoter (*promTCP4:wtTCP4:GFP* and *promTCP4:rTCP4:GFP*, respectively). The *promTCP4:rTCP4:GFP* construct was expressed at low levels in roots, mostly in the stele, but also in the epidermis and lateral root cap, including the initial cells for these tissues (8 out of 10 plants) (Fig. 3e, f). By contrast, we were not able to detect fluorescent signal in *promTCP4:wtTCP4:GFP* plants (25 out of 25 plants; Figs. 3g, h; S5), suggesting a tight control by miR319 on *TCP4* expression in the root. Not surprisingly, we observed

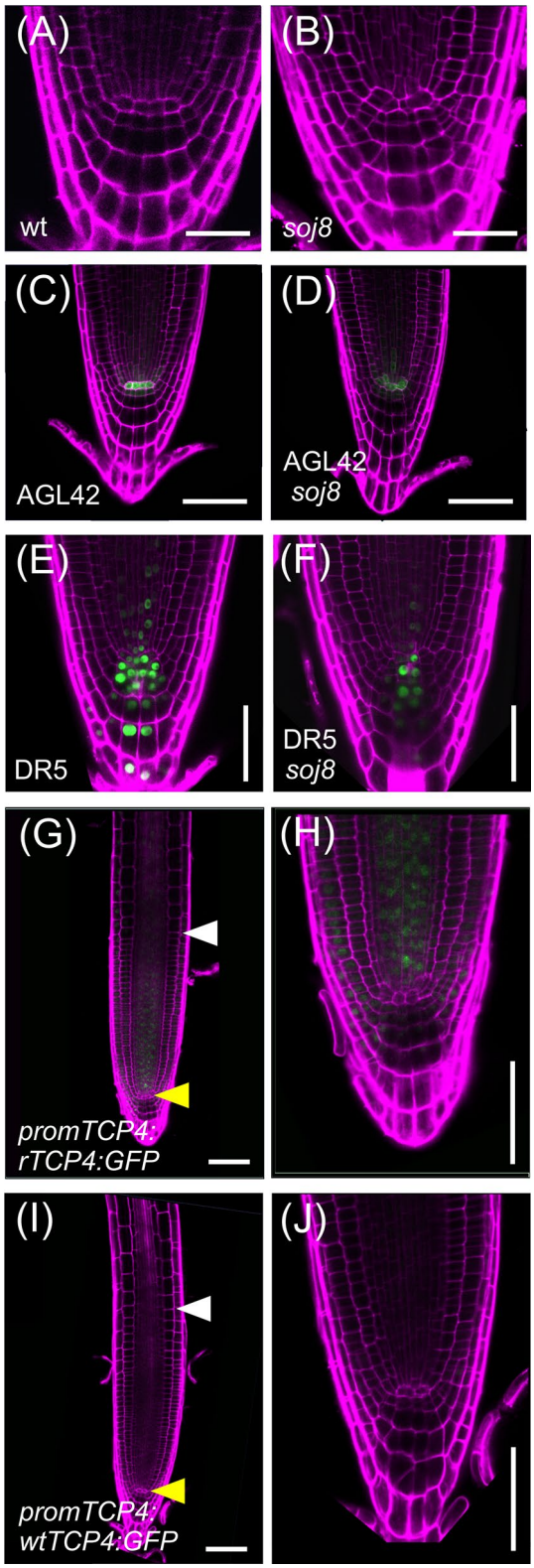

Fig. 3 Increased TCP4 levels affect the cellular organization of the RAM. **a**–**h** Representative confocal images of propidium iodide-stained (magenta) root tips. **a** wt, notice the normal QC (23 of 25 observed roots). **b** *soj8*, notice the disturbed QC (43 of 61 observed roots). **c** *promAGL42:GFP* reporter line, notice expression in QC cells. **d** *promAGL42:GFP* reporter line crossed with *soj8* mutant, notice altered expression pattern. **e**–**f** *DR5:3xVENUS-N7* reporter line (image representative for 13 observed individuals) and *DR5:3xVENUS-N7* reporter in *soj8* mutant background (image representative for 16 analyzed individuals). **g**–**h** *promTCP4:rTCP4:GFP* (image representative for 8 out of 10 analyzed individuals). **i**–**j** *promTCP4:wtTCP4:GFP* (image representative for 25 out of 25 analyzed individuals). Scale bars: 20 µm for (**a**, **b**) and 50 µm for (**c**–**h**). In **e** and **g**, white arrowheads indicate the end of the MZ, and yellow ones mark the QC. Separate PI and GFP channels and merged images are shown in Fig. S5

distorted QCs in the *promTCP4:rTCP4:GFP* plants, similar to those in the *soj8* mutant, while the QCs of the *promTCP4:wtTCP4:GFP* plants seemed normal (Figs. 3e–h, S1).

High levels of TCP2 also affect root growth and meristem organization

To further characterize the role of miR319 in roots, we turned to *TCP2*, another miR319-regulated *TCP*, the overexpression of which has weaker effects compared to TCP4 (Palatnik et al. 2003). We transformed plants with a wild-type *TCP2* (*prom35S:wtTCP2:GFP*) and a microRNA-resistant *TCP2* (*prom35S:rTCP2:GFP*) construct (Fig. 4a) along with an empty vector control. Even though several of the primary transformants did not set seeds we were able to select nine independent lines for the first construct and six for the second, and five lines carrying the empty vector that we used as control. We measured root length in young seedlings and found that, whereas the *prom35S:wtTCP2:GFP* lines showed no difference from the control, those lines expressing *prom35S:rTCP2:GFP* did have significantly shorter roots seven days after germination (Fig. 4b). We confirmed for one of the stronger *prom35S:rTCP2:GFP* lines that the transcript levels of *TCP2* were strongly increased, whereas at the same time the expression of *CYCB1;2* was reduced (Fig. S6). Therefore, we conclude that lifting microRNA control from *TCP2* expression can also reduce root length in Arabidopsis.

We also analyzed the RAM of *prom35S:wtTCP2:GFP* and *prom35S:rTCP2:GFP* as well as control plants. We found that almost all (12 of 13) analyzed independent transgenic *prom35S:wtTCP2:GFP* plants had a normal RAM and very low fluorescent signal (Figs. 4c, d; S7). Opposingly, 47% of the *prom35S:rTCP2:GFP* individuals (15 of 32) had distorted RAMs: 34% mildly (11 of 32; Figs. 4e; S7) and 13% severely (4 of 32; Figs. 4f; S7). Plants with strong phenotypes turned out sterile and hence did not allow for analysis in the following generations. However, from the individuals that did set seeds we chose three for each construct and confirmed the persistence of RAM defects in the following generations (Fig. S8).

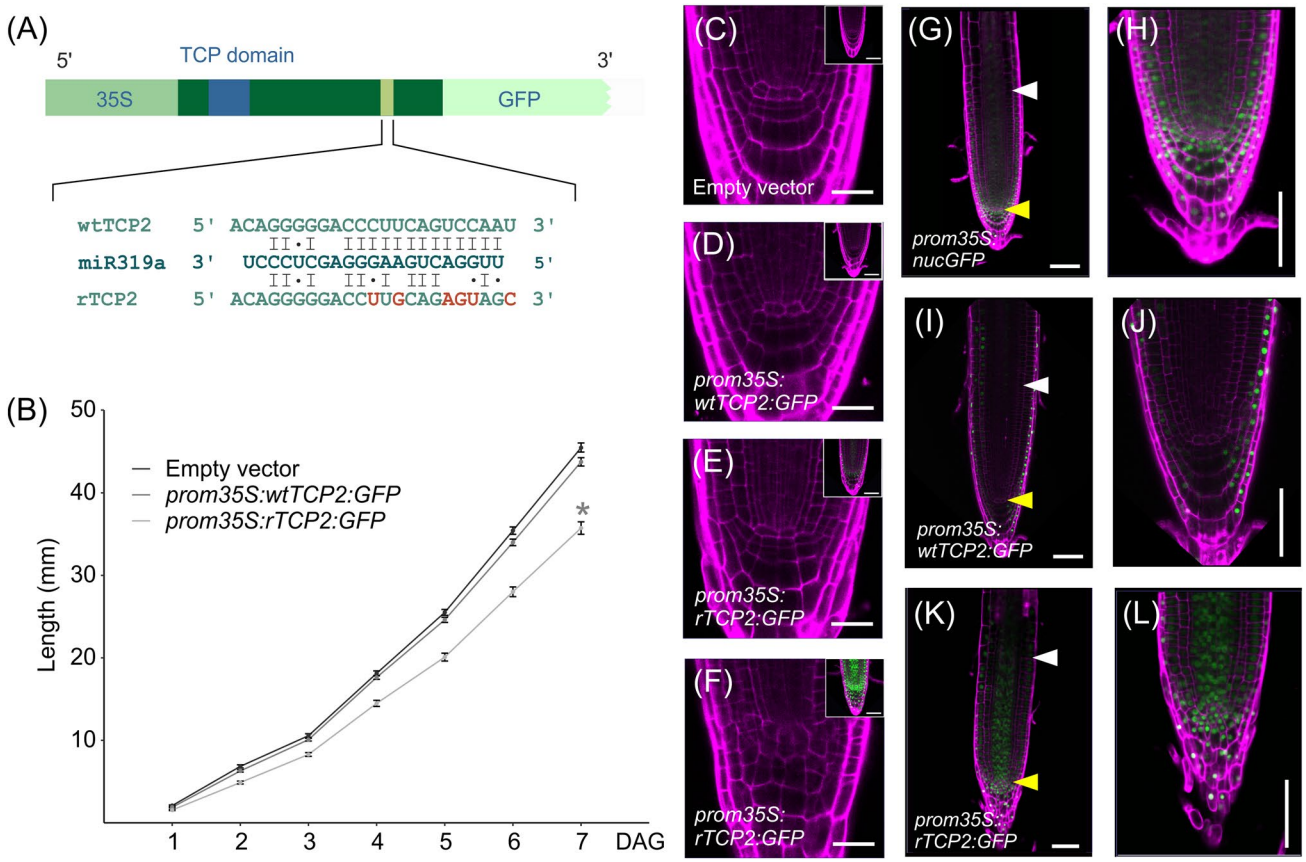

Fig. 4 Excess of TCP2 affects root growth and RAM organization. **a** Schematic representation of the *TCP2:GFP* constructs. Dark green box indicates coding region with TCP domain highlighted in blue and miR319 target site in olive green; 35S promoter and GFP are indicated by lighter green boxes. **b** Line plot showing mean root length of independent transgenic lines for *prom35S:wtTCP2:GFP*, *prom35S:rTCP2:GFP* and empty vector control. X-axis is days after germination (DAG). The line for each transgenic construct represents the mean for all analyzed individual lines (nine lines for *prom35S:wtTCP2:GFP*, six lines for *prom35S:rTCP2:GFP* and five lines for empty vector). The average of each independent line was taken as a single datum; out of these, new means and standard errors were calculated and plotted. Asterisk indicates significant difference at seven DAG for *prom35S:rTCP2:GFP* from empty vector control (ANOVA, $p < 0{,}01$). **c–f** Representative confocal images showing PI detecting channel (and merged image of PI and GFP detecting channel in inset) of QCs for: control (**c**), *prom35S:wt:TCP2:GFP* (**d**), *prom35S:r:TCP2:GFP* with mild distortion of QC as observed in 34% of plants (**e**) and *prom35S:r:TCP2:GFP* with severely distorted QC as observed in 13% of plants (**f**). **g–l** GFP expression in the RAM of *35S:nuclearGFP* control (**g–h**), *prom35S:wtTCP2:GFP* (**i–j**) and *prom35S:rTCP2:GFP* (**k–l**). In **g**, **I** and **k**, white arrowheads indicate the end of the MZ, and yellow ones mark the QC. Scale bars: c-f 20 µm, **g–l** 50 µm. Separate PI and GFP channels and merged images are shown in Fig. S7

We further used the *prom35S:wtTCP2:GFP* and *prom35S:rTCP2:GFP* lines to assess miR319 activity in the root. After confirming homogenous and ubiquitous activity of the promoter in root tissues with a *prom35S:nuclearGFP* control vector (Figs. 4g, h; S7) we analyzed the *prom35S:rTCP2:GFP* primary transformants and found GFP expression throughout the RAM as expected (Figs. 4k, l; S7). However, GFP expression from *prom35S:wtTCP2:GFP* roots was much weaker and could only be detected in the epidermis, cortex, lateral root cap and the tip of the columella, but not in the stele, endodermis or QC (20 out of 25 plants; Figs. 4i, j; S7), suggesting that miR319 may act in all dividing tissues in the RAM and is able to regulate *TCP2*, and most likely the other TCPs with an miR319 target site as well.

miR319 functions in different ways in leaves and roots

To conclude, we decided to compare leaf and root phenotypes of the *soj8* mutant where *TCP4* activity partially escapes miR319 control with those of plants that have reduced TCP levels. We used individual and subsequent combinations of loss-of-function alleles for four out of five miR319-regulated TCPs, and the miR319-overexpressing *jaw*-D mutant in which all of them are down-regulated. As

previously observed (Palatnik et al. 2003; Schommer et al. 2008), simple, and multiple *tcp* knock-out lines as well as the *jaw*-D mutant, exhibit changes that range from a slight increase in leaf size to extensive alterations in leaf shape, while *soj8* presented opposite aerial phenotypes (Fig. 5a). However, when we analyzed the roots of the different *tcp* mutants and *jaw*-D, we saw no difference in length compared to wild-type roots (Fig. 5a, b). In good agreement, an analysis of publicly available data sets describing gene expression in root confirmed that miR319 regulated *TCP*s are not detected or expressed at very low levels in this organ (Fig. S9) (Brady et al. 2007; Tsukagoshi et al. 2010; Klepikova et al. 2016). These results suggest that miR319-regulated *TCPs* do not have an obvious function during normal root growth in Arabidopsis, but that it is rather necessary to keep them under the post-transcriptional control exerted by the microRNA.

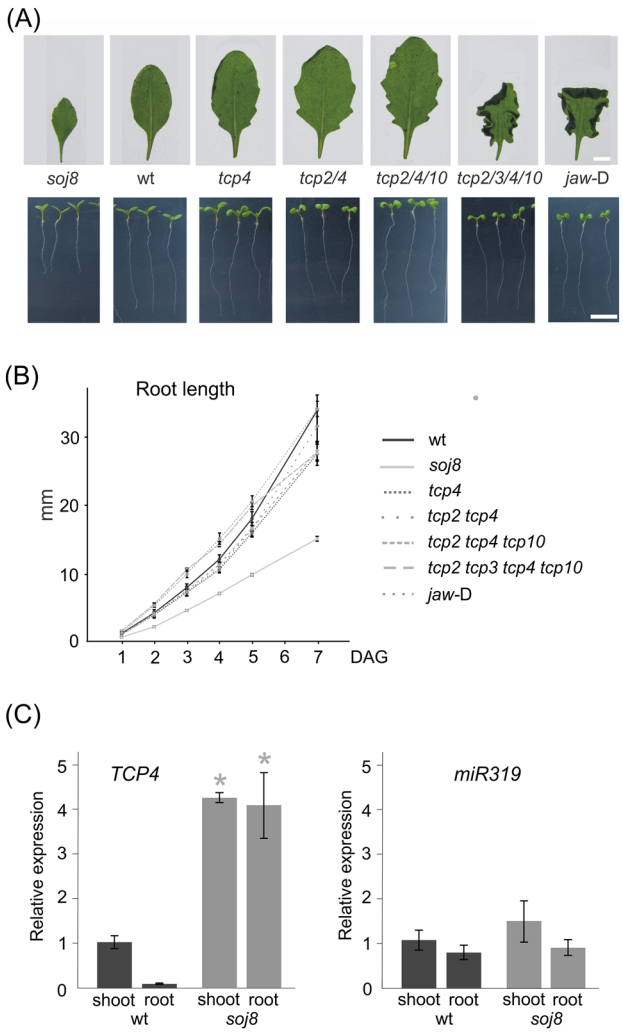

Fig. 5 Reduction of TCP activity does not affect root growth. **a** Leaf and root phenotypes of mutant lines with decreasing TCP activity. Upper panels: 5th rosette leaf; lower panels: seedlings grown vertically for five days. Scale bar: 1 cm. **b** Root length in different *tcp* mutants and *jaw*-D mutant compared to wild type, until seven days after germination (DAG). **c** Relative expression levels of *TCP4* mRNA and mature miR319 in wild-type and *soj8* shoot apices and roots. Asterisks indicate significant differences in *soj8* from wildtype as determined by Student's t-test ($p < 0.01$)

We measured mature miR319 and *TCP4* transcript levels in 5-day-old root tips and shoot apices of wild-type and *soj8* plants by RT-qPCR (Fig. 5c). In wild type, *TCP4* transcript levels were more than 10 times higher in shoot than root apices. Then, we analyzed *TCP4* transcript levels in *soj8* and found an increase of approximately four times in the apex compared to wild type. Surprisingly, when we measured *TCP4* transcript levels in *soj8* roots, we found an increase of more than ten times with respect to wild-type plants, indicating that mis-regulation of *TCP4* due to a mutation in the miR319 target site has a larger relative impact on root than on shoot apices. Interestingly, *TCP4* transcript levels were similar in *soj8* shoots and roots, suggesting that the promoter has a similar strength in both, but that the miR319-regulation has a different contribution in these two tissues. Our results suggest that, while the miR319/TCP quantitative balance regulates leaf development, the miRNA functions as a potent inhibitor of *TCP* expression in roots.

Discussion

In both plants and animals, microRNA circuits include the clearance and/or potent inhibition of their target RNAs, as well as the dampening and/or fine-tuning of target gene expression (Flynt and Lai 2008; Voinnet 2009). Here, we found that the miR319 regulatory network operates through different modes in shoots and roots. In opposition to what is seen in the shoot, we have shown that reduced levels of microRNA-regulated TCPs have no effect on root growth, and only escape from microRNA control and therefore increased activity impairs the organ's growth. Given our observations and taking into consideration the high miR319 activity in root tissue, as shown in other reports (Ghosh Dastidar et al. 2016), and low *TCP4* levels in wild-type roots, we conclude that miR319 regulates the *TCP*s by two contrasting mechanisms: in the shoot, it quantitatively regulates, i.e. fine-tunes them to achieve proper size and shape of the organs; In roots, however, it qualitatively regulates, and potently inhibits its targets preventing them from interfering with correct growth and architecture of the organ. Interestingly, miR159 has been shown to completely silence its targets *MYB33* and *MYB65* in vegetative tissues while quantitatively repressing them in aleurone and the embryo of germinating seeds (Alonso-Peral et al. 2012).

Furthermore, in this study we provide new insights about the role of the miR319-TCP regulatory node in the Arabidopsis root. We characterized the *soj8* mutant line, which

exhibits impaired regulation by miR319 resulting in higher TCP4 activity. We found that increased TCP activity in the root had effects on both, root growth and QC cellular architecture. On one hand it slowed down elongation and shortened the root. On the other hand, at the cellular level, it disrupted the normal RAM architecture and reduced cell proliferation, as judged by *CYCB* expression. This resulted in a meristem with fewer cells but did not affect the final length of the mature cortex cells.

Formation of different TCP protein-complexes has been shown to regulate leaf complexity (Rubio-Somoza et al. 2014). It is possible that in the *soj8* root unbalanced TCP levels result in the generation of different protein-complexes. Even a direct competition of the microRNA-regulated class II TCP4 with class I TCPs, which can have opposite effects (Koyama et al. 2010; Ichihashi et al. 2011; Uberti-Manassero et al. 2012) for their position in protein complexes might be possible. For instance, class I TCP20 interacts with SCARECROW and PLETHORA (Shimotohno et al. 2018), two QC organizers, and should it be replaced by TCP4, the function of the resulting protein complex might be compromised.

TCP transcription factors participate in various developmental processes and regulate genes involved in the biosynthesis and activity of phytohormones (Schommer et al. 2008; Koyama et al. 2010), some of which are important in establishing and maintaining the root stem cell niche (Dello Ioio et al. 2008; Chen et al. 2011). TCP3 and TCP15 directly bind to the promoter of *SHY2*. Interestingly, the class II TCP3, the closest related family member to TCP4, promotes *SHY2* expression, while TCP15, a class I member of the family, represses it (Koyama et al. 2010; Ichihashi et al. 2011; Uberti-Manassero et al. 2012). *SHY2* is a key integrator of auxin and cytokinin response in the root (Dello Ioio et al. 2008) and contributes to maintain the size of the root meristematic zone. Therefore, hyperactivation of *SHY2* in the *soj8* background might imbalance the hormonal setting, resulting in abnormal root growth. Interestingly, the expression of a DR5 auxin reporter line is reduced in the stem cell niche region in *soj8* mutant background which strengthens the idea of an imbalanced hormonal setting upon the deregulation of *TCP4*. One important integrator of the auxin signal in the root is the homeodomain transcription factor WOX5, which is expressed in the QC where it avoids cell division. From there it moves to the columella stem cells and prevents their differentiation. Therefore, it would be interesting to test if WOX5 expression is affected in the *soj8* mutant background and at the base of the observed root defects. Another TCP target up-regulated in *soj8* is *LOX2*, an enzyme involved in JA biosynthesis. This hormone inhibits primary root growth in Arabidopsis and decreases mitotic activity of the RAM, leading to irregular QC divisions and premature differentiation of the columella stem cells, which in turn originate altered daughter cells (Chen et al. 2011). It has also been shown that wound-induced production of JA can stimulate CYCD6;1 in the root stem cell niche (Zhou et al. 2019a).

Notably, *soj8* appears to show a combination of the two phenotypes described for the dominant mutant *shy2-2* and for JA-treated plants. Based on the clear *SHY2* and *LOX2* induction, we propose that the morphological and functional changes in *soj8* could reflect the joint alteration of phytohormone pathways, although this would require further confirmatory work. All in all, our results provide new insights into the importance of the miR319-TCP regulatory node during Arabidopsis root growth and highlight that the same microRNA can operate through different modes, target clearance or fine-tuning depending on the cellular context.

Supplementary Information The online version contains supplementary material available at https://doi.org/10.1007/s11103-021-01227-8.

Acknowledgements We thank Ramiro Rodriguez for helpful discussions and Rodrigo Vena for technical assistance in image acquisition. EGB, JLB and CG were supported by fellowships from CONICET. JFP and CS are members of CONICET. This work was supported by Grants to JFP (ICGEB CRP/ARG17-01) and CS (Project: IO-345-17 of Agencia Santafesina de Ciencia Tecnología e Innovación and project: PICT 2019-03571 of Agencia Nacional de Promoción de la Investigación, el Desarrollo Tecnológico y la Innovación).

Author contributions EGB, JLB, CG and CS performed the experiments. EGB, JFP and CS conceived the experiments. EGB, JLB, JFP and CS wrote the manuscript.

Funding EGB, JLB and CG were supported by fellowships from CONICET. JFP and CS are members of CONICET. This work was supported by Grants to JFP (ICGEB CRP/ARG17-01) and CS (Project: IO-345-17 of Agencia Santafesina de Ciencia Tecnología e Innovación; and project: PICT 2019-03571 of Agencia Nacional de Promoción de la Investigación, el Desarrollo Tecnológico y la Innovación).

Data availability Vectors and mutant lines generated in this study are available on request.

Code availability Not applicable.

Declarations

Conflict of interest The authors declare that the research was conducted in the absence of any commercial or financial relationships that could be construed as a potential conflict of interest.

References

Alonso-Peral MM, Sun C, Millar AA (2012) MicroRNA159 can act as a switch or tuning microRNA independently of its abundance in Arabidopsis. PLoS ONE 7:e34751

Bao M, Bian H, Zha Y, Li F, Sun Y, Bai B, Chen Z, Wang J, Zhu M, Han N (2014) miR396a-mediated basic helix-loop-helix transcription factor bHLH74 repression acts as a regulator for root growth in Arabidopsis seedlings. Plant Cell Physiol 55:1343–1353

Bell E, Creelman RA, Mullet JE (1995) A chloroplast lipoxygenase is required for wound-induced jasmonic acid accumulation in Arabidopsis. Proc Natl Acad Sci U S A 92:8675–8679

Brady SM, Orlando DA, Lee JY, Wang JY, Koch J, Dinneny JR, Mace D, Ohler U, Benfey PN (2007) A high-resolution root spatiotemporal map reveals dominant expression patterns. Science 318:801–806

Bresso EG, Chorostecki U, Rodriguez RE, Palatnik JF, Schommer C (2018) Spatial control of gene expression by miR319-regulated TCP transcription factors in leaf development. Plant Physiol 176:1694–1708

Chen C, Ridzon DA, Broomer AJ, Zhou Z, Lee DH, Nguyen JT, Barbisin M, Xu NL, Mahuvakar VR, Andersen MR, Lao KQ, Livak KJ, Guegler KJ (2005) Real-time quantification of microRNAs by stem-loop RT-PCR. Nucleic Acids Res 33:e179

Chen Q, Sun J, Zhai Q, Zhou W, Qi L, Xu L, Wang B, Chen R, Jiang H, Qi J, Li X, Palme K, Li C (2011) The basic helix-loop-helix transcription factor MYC2 directly represses PLETHORA expression during jasmonate-mediated modulation of the root stem cell niche in Arabidopsis. Plant Cell 23:3335–3352

Citerne HL, Luo D, Pennington RT, Coen E, Cronk QC (2003) A phylogenomic investigation of CYCLOIDEA-like TCP genes in the Leguminosae. Plant Physiol 131:1042–1053

Clough SJ, Bent AF (1998) Floral dip: a simplified method for Agrobacterium-mediated transformation of *Arabidopsis thaliana*. Plant J 16:735–743

Colon-Carmona A, You R, Haimovitch-Gal T, Doerner P (1999) Technical advance: spatio-temporal analysis of mitotic activity with a labile cyclin-GUS fusion protein. Plant J 20:503–508

Cubas P, Lauter N, Doebley J, Coen E (1999) The TCP domain: a motif found in proteins regulating plant growth and development. Plant J 18:215–222

Danisman S, van Dijk AD, Bimbo A, van der Wal F, Hennig L, de Folter S, Angenent GC, Immink RG (2013) Analysis of functional redundancies within the Arabidopsis TCP transcription factor family. J Exp Bot 64:5673–5685

Dello Ioio R, Nakamura K, Moubayidin L, Perilli S, Taniguchi M, Morita MT, Aoyama T, Costantino P, Sabatini S (2008) A genetic framework for the control of cell division and differentiation in the root meristem. Science 322:1380–1384

Donnelly PM, Bonetta D, Tsukaya H, Dengler RE, Dengler NG (1999) Cell cycling and cell enlargement in developing leaves of Arabidopsis. Dev Biol 215:407–419

Efroni I, Blum E, Goldshmidt A, Eshed Y (2008) A protracted and dynamic maturation schedule underlies Arabidopsis leaf development. Plant Cell 20:2293–2306

Ercoli MF, Vena R, Goldy C, Palatnik JF, Rodriguez RE (2018a) Analysis of expression gradients of developmental regulators in *Arabidopsis thaliana* roots. Methods Mol Biol 1863:3–17

Ercoli MF, Ferela A, Debernardi JM, Perrone AP, Rodriguez RE, Palatnik JF (2018b) GIF transcriptional coregulators control root meristem homeostasis. Plant Cell 30:347–359

Flynt AS, Lai EC (2008) Biological principles of microRNA-mediated regulation: shared themes amid diversity. Nat Rev Genet 9:831–842

Ghosh Dastidar M, Mosiolek M, Bleckmann A, Dresselhaus T, Nodine MD, Maizel A (2016) Sensitive whole mount in situ localization of small RNAs in plants. Plant J 88:694–702

Heisler MG, Ohno C, Das P, Sieber P, Reddy GV, Long JA, Meyerowitz EM (2005) Patterns of auxin transport and gene expression during primordium development revealed by live imaging of the Arabidopsis inflorescence meristem. Curr Biol 15:1899–1911

Ichihashi Y, Kawade K, Usami T, Horiguchi G, Takahashi T, Tsukaya H (2011) Key proliferative activity in the junction between the leaf blade and leaf petiole of Arabidopsis. Plant Physiol 157:1151–1162

Jarvis P, Chen LJ, Li H, Peto CA, Fankhauser C, Chory J (1998) An Arabidopsis mutant defective in the plastid general protein import apparatus. Science 282:100–103

Klepikova AV, Kasianov AS, Gerasimov ES, Logacheva MD, Penin AA (2016) A high resolution map of the Arabidopsis thaliana developmental transcriptome based on RNA-seq profiling. Plant J 88:1058–1070

Koyama T, Mitsuda N, Seki M, Shinozaki K, Ohme-Takagi M (2010) TCP transcription factors regulate the activities of ASYMMETRIC LEAVES1 and miR164, as well as the auxin response, during differentiation of leaves in Arabidopsis. Plant Cell 22:3574–3588

Li S (2015) The *Arabidopsis thaliana* TCP transcription factors: a broadening horizon beyond development. Plant Signal Behav 10:e1044192

Lucas JR, Shaw SL (2012) MAP65-1 and MAP65-2 promote cell proliferation and axial growth in Arabidopsis roots. Plant J 71:454–463

Martin-Trillo M, Cubas P (2010) TCP genes: a family snapshot ten years later. Trends Plant Sci 15:31–39

Nawy T, Lee JY, Colinas J, Wang JY, Thongrod SC, Malamy JE, Birnbaum K, Benfey PN (2005) Transcriptional profile of the Arabidopsis root quiescent center. Plant Cell 17:1908–1925

Palatnik JF, Allen E, Wu X, Schommer C, Schwab R, Carrington JC, Weigel D (2003) Control of leaf morphogenesis by microRNAs. Nature 425:257–263

Palatnik JF, Wollmann H, Schommer C, Schwab R, Boisbouvier J, Rodriguez R, Warthmann N, Allen E, Dezulian T, Huson D, Carrington JC, Weigel D (2007) Sequence and expression differences underlie functional specialization of Arabidopsis microRNAs miR159 and miR319. Dev Cell 13:115–125

Petricka JJ, Winter CM, Benfey PN (2012) Control of Arabidopsis root development. Annu Rev Plant Biol 63:563–590

Rubio-Somoza I, Zhou CM, Confraria A, Martinho C, von Born P, Baena-Gonzalez E, Wang JW, Weigel D (2014) Temporal control of leaf complexity by miRNA-regulated licensing of protein complexes. Curr Biol 24:2714–2719

Schindelin J, Arganda-Carreras I, Frise E, Kaynig V, Longair M, Pietzsch T, Preibisch S, Rueden C, Saalfeld S, Schmid B, Tinevez JY, White DJ, Hartenstein V, Eliceiri K, Tomancak P, Cardona A (2012) Fiji: an open-source platform for biological-image analysis. Nat Methods 9:676–682

Schommer C, Palatnik JF, Aggarwal P, Chetelat A, Cubas P, Farmer EE, Nath U, Weigel D (2008) Control of jasmonate biosynthesis and senescence by miR319 targets. PLoS Biol 6:e230

Schommer C, Debernardi JM, Bresso EG, Rodriguez RE, Palatnik JF (2014) Repression of cell proliferation by miR319-regulated TCP4. Mol Plant 7:1533–1544

Shimotohno A, Heidstra R, Blilou I, Scheres B (2018) Root stem cell niche organizer specification by molecular convergence of PLETHORA and SCARECROW transcription factor modules. Genes Dev 32:1085–1100

Tian Q, Uhlir NJ, Reed JW (2002) Arabidopsis SHY2/IAA3 inhibits auxin-regulated gene expression. Plant Cell 14:301–319

Tsukagoshi H, Busch W, Benfey PN (2010) Transcriptional regulation of ROS controls transition from proliferation to differentiation in the root. Cell 143:606–616

Uberti-Manassero NG, Lucero LE, Viola IL, Vegetti AC, Gonzalez DH (2012) The class I protein AtTCP15 modulates plant development through a pathway that overlaps with the one affected by CIN-like TCP proteins. J Exp Bot 63:809–823

Voinnet O (2009) Origin, biogenesis, and activity of plant microRNAs. Cell 136:669–687

Weigel D, Glazebrook J (2009) Quick miniprep for plant DNA isolation. Cold Spring Harb Protoc 2009, pdb prot5179.

Wen B, Nieuwland J, Murray JA (2013) The Arabidopsis CDK inhibitor ICK3/KRP5 is rate limiting for primary root growth and

promotes growth through cell elongation and endoreduplication. J Exp Bot 64:1135–1144

Zhou W, Lozano-Torres JL, Blilou I, Zhang X, Zhai Q, Smant G, Li C, Scheres B (2019a) A jasmonate signaling network activates root stem cells and promotes regeneration. Cell 177(942–956):e914

Zhou Y, Xun Q, Zhang D, Lv M, Ou Y, Li J (2019b) TCP transcription factors associate with PHYTOCHROME INTERACTING FACTOR 4 and CRYPTOCHROME 1 to regulate thermomorphogenesis in *Arabidopsis thaliana*. iScience 15:600–610